

Correlated two-photon imaging with true thermal light

Da Zhang¹, Xi-Hao Chen^{1,2}, Yan-Hua Zhai¹, and Ling-An Wu¹

¹*Institute of Physics, Chinese Academy of Sciences, Beijing 100080*

²*Department of Physics, Liaoning University, Shenyang 110036, China*

We report the first experimental demonstration of two-photon correlated imaging with true thermal light from a hollow cathode lamp. The coherence time of the source is much shorter than that of previous experiments using random scattered light from a laser. A two-pinhole mask was used as object, and the corresponding thin lens equation was well satisfied. Since thermal light sources are easier to obtain and measure than entangled light it is conceivable that they may be used in special imaging applications.

Although imaging is an old and well-studied topic and is of great importance in classical optics, it is now attracting new interest in quantum optics due to recent experiments on two-photon correlated imaging. The first such experiment was based on quantum entangled photon pairs from spontaneous parametric down conversion in a nonlinear crystal, and gave rise to the name “ghost” imaging, so called because an object in one optical beam could produce an image in the coincident counts with a detector placed in another beam [1]. This experiment led to other interesting theoretical and experimental studies and, furthermore, a debate on the question whether entanglement is a prerequisite for ghost imaging [2]. The possibility to perform correlated imaging with thermal light was first predicted by Gatti et al [4]. The first experiment with a classical light source that demonstrated “two photon” coincidence imaging was performed by Bennink et al. using a coherent laser beam split along two paths with detectors that measured finite laser pulses [3].

The difference between quantum and classical coincidence imaging and the extent to which a classical light source can mimic a quantum one have been widely discussed by the groups of Shih [5, 6], Boyd [7], Lugiatto [4, 8, 9], Zhu [10, 11] and Wang [12]. Experimentally, Shih and collaborators first achieved ghost imaging with a pseudo-thermal light source, and introduced the concepts of “two-photon coherence” and “two-photon incoherence” imaging [13]. Gatti et al. obtained high resolution ghost imaging with thermal-like speckle light. However, in all these experiments the primary light source was a He-Ne laser, and the pseudo-thermal beam was obtained by passage through a rotating ground glass plate [14].

Different from these experiments, we report the demonstration of a two-photon correlated imaging experiment using a true thermal light source.

We employed a commercial rubidium hollow-cathode lamp [16] manufactured by the General Research Institute for Nonferrous Metals (China), which is the type commonly used in atomic absorption spectroscopy because of its sharp spectral linewidth. The lamp was powered by a direct current of 20mA in our experiments, and the resonance wavelength was 780nm. However, the actual linewidth of hollow-cathode lamps depends on the pressure, filament structure etc and varies from model to

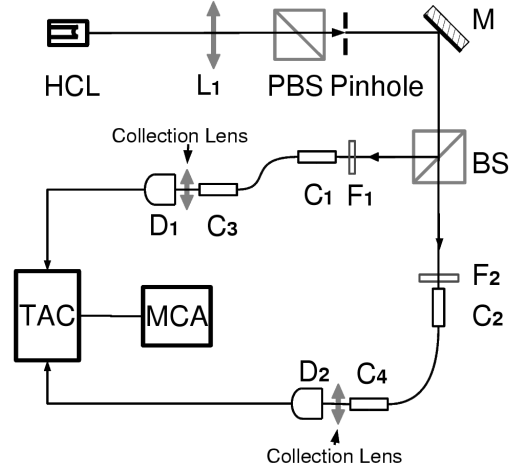


FIG. 1: Schematic of the HBT type experiment. HCL: hollow cathode lamp; L_1 : lens of focal length 10cm; pinhole diameter: 0.5mm; effective diameter of collimators is 2mm.

model. In our model the inner diameter of the cathode was 3mm. To estimate the coherence time of our lamp we first carried out a Hanbury Brown-Twiss (HBT) type experiment, with the setup shown schematically in Fig. 1. The light from the lamp is focused by the convex lens (L_1) of 10cm focal length onto a circular pinhole 0.5mm in diameter to form a secondary light source. A polarizing beam splitter (PBS) in front of the pinhole transmits linearly polarized light. After reflection by a mirror (M) the beam is divided by a 50%/50% non-polarizing beam splitter (BS). The reflected and transmitted beams pass through interference filters F_1 and F_2 before being coupled into single photon detectors D_1 and D_2 , respectively, through fiber collimators C_1 and C_2 . The transmission of the interference filters is about 70% at 780nm and the receiving area of the collimators is about 2mm in diameter. The detector output signals are sent to a time-amplitude converter (TAC), with D_1 and D_2 providing the “start” and “stop” signals, respectively. The TAC output is connected to a multi-channel analyzer (MCA), and the computer displays a histogram of the different intervals between the times of arrival of the photons at

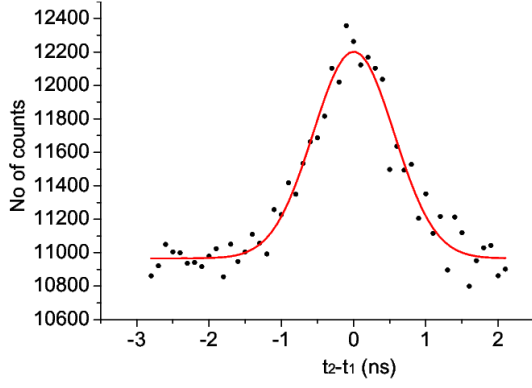


FIG. 2: Number of counts vs time interval for the HBT type experiment. The solid curve is a Gaussian fit of data points. The FWHM of the peak is about 1.3ns which is due to the time jitter of the electronic circuits.

the two detectors. From this we obtain the relation between the photon count rate and time interval, and subsequently the second-order correlation function

$$G^{(2)}(t_2 - t_1) = \langle \hat{E}_2(t_2)^{-} \hat{E}_1(t_1)^{-} \hat{E}_1(t_1)^{+} \hat{E}_2(t_2)^{+} \rangle,$$

here $\hat{E}_i^{(-)}(t_i)$ are the positive and negative frequency field operators at detectors $D_i (i = 1, 2)$ at time t_i , respectively. The normalized second-order correlation function $g^{(2)}(t_2 - t_1)$, which describes the intensity correlation of a light field at two detectors [17], is given by

$$g^{(2)}(t_2 - t_1) = \frac{G^{(2)}(t_2 - t_1)}{G_1^{(1)}(t_1)G_1^{(1)}(t_2)}, \quad (1)$$

If the average intensity of the light remains constant [18],

$$\lim_{(t_2 - t_1) \rightarrow \infty} G^{(2)}(t_2 - t_1) = I_1 I_2 = G_1^{(1)}(t_1) G_2^{(1)}(t_1).$$

we obtain the value $g^{(2)}(t_2 - t_1 = 0)$ experimentally by dividing the values of the average $G^{(2)}(t_2 - t_1)$ for values of, $|t_2 - t_1| \leq 0.25ns$ (the width of the coincidence window) by the value of $G^{(2)}(t_2 - t_1)$ for $|t_2 - t_1| \gg 1.3ns$ (corresponding to signals arriving randomly beyond any correlation time).

A typical set of data from our experiment is shown in Fig. 2. The full width at half maximum (FWHM) of the peak is about 1.3ns, which is much longer than the coherence time of the light, and is mainly due to the time jitter in the electronic circuits. From the above data we derive the coherence time τ_0 to be about 0.2ns [15], which is much shorter than that of previous experiments using randomly scattered light from a He-Ne laser. The maximum of the measured normalized second-order correlation function $g^{(2)}$ is 1.11, corresponding to a maximum visibility of about 5%. The deviation of the measured $g^{(2)}$ from the theoretical value 2 is due to the area of the non-point-like collimator, as well as the time jitter of the

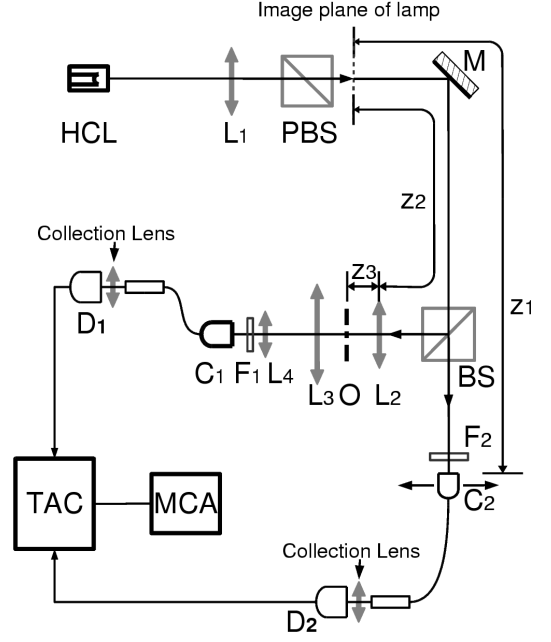


FIG. 3: Experimental set-up of the ghost imaging experiment. Focal length of $L_2 = 20cm$, $z_1 - z_2 = 32.5cm$, $z_3 = 12.4cm$, $z_1 = 1.8m$; the image of the cathode $\approx 1mm$ in diameter.

electronic circuits. When we increased the area of the light source (the size of the pinhole), the value of $g^{(2)}$ decreased further, as expected.

For our correlated ghost imaging experiment the set-up in the HBT type experiment is modified as shown in Fig. 3. The pinhole in the image plane of the lamp is removed for greater light throughput. The object, a mask (O) consisting of two pinholes, is inserted in the beam reflected from the beamsplitter BS. The diameter of both pinholes is 0.5mm and the distance between them is 1.3mm. Two lenses L_3 and L_4 act as a telescope so that D_1 can capture all the light passing through the mask and serve as a bucket detector. The third lens L_2 inserted between the beam splitter and the mask is the convex imaging lens, and has a focal length of about 20cm. Note that this set-up is different from those of references 4 and 6, and the corresponding Gaussian thin lens equation is

$$\frac{1}{z_2 - z_1} + \frac{1}{z_3} = \frac{1}{f}, \quad (2)$$

where z_1 and z_2 are the distances from collimator C_2 and lens L_2 to the secondary light source, respectively, and z_3 is the distance from lens L_2 to the mask O; f is the focal length of L_2 . This equation can be found in references [11, 12] for incoherent ghost imaging, and is the same as that for quantum ghost imaging [1], except that $+z_1$ is replaced by $-z_1$.

The transverse normalized second-order correlation function is given by [13]:

$$g^{(2)}(x_2) \propto N + |T(\frac{z_3}{z_1 - z_2} x_2)|^2, \quad (3)$$

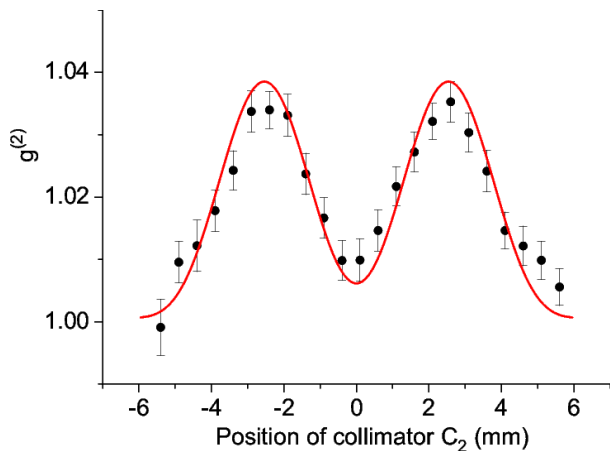


FIG. 4: Dependence of the normalized second order correlation function $g^{(2)}$ on the position of fiber collimator C_2 , which gives the cross sectional image of the two pinholes. The solid curve is calculated taking into consideration the finite size of the detectors [19].

where x_2 is the transverse position of fiber collimator C_2 , $T(x)$ the transmission function of the mask (O), and N the number of transparent features in the object plane, which equals 2 in our scheme because there are two pinholes in the mask. This equation reflects the position-position correlation between the object and image planes, as well as the fact that the visibility decreases (background increases) when the number of points in the object increases.

In our experiment we choose the case of the object distance $z_3 < f$ [12], with $z_3 = 12.4\text{cm}$ and image distance $z_1 - z_2 = 32.5\text{cm}$. The fiber collimator C_2 is scanned transversely across the reference beam in steps of 0.5mm ,

and the detector coincidence counts recorded as above for the HBT type experiment. The actual single count rates of D_1 and D_2 were about 300k/sec , and about 30k counts were accumulated for each data point. The normalized second-order correlation function $g^{(2)}$ was calculated as above, from which we plot the cross sectional image of the two-pinhole object, as shown in Fig. 4. The visibility is found to be 2%.

Apart from the factor N in Eq. 3, other reasons for the lower visibility include the short coherence time compared with the time jitter of the detection system, the limited coherence area in the object plane, which is affected by the area of light source, and the finite area of the fiber collimator C_2 . The low resolution is due to the finite area of scanning fiber collimator and the finite coherence area in the object plane, which is about 0.35mm^2 .

In conclusion, we have experimentally realized ghost imaging with true thermally incoherent light, showing that thermal light can emulate the role of entangled light in ghost imaging experiments to a certain extent. Although the visibility is very low this could be greatly improved by removing the background by some means, e.g. digitally. Since thermal light sources are easier to obtain and measure it is conceivable that they could find certain special applications [20] where entangled sources are not so convenient to use.

We are grateful to Yan-Hua Shih, De-Zhong Cao, Kai-ge Wang, and Shi-Yao Zhu for useful discussions. We also thank Zhan-Chun Zuo and Hai-Qiang Ma for their experimental assistance. This work was supported by the National Natural Science Foundation of China (Grant No. 60178013) and the Knowledge Innovation Program of the Chinese Academy of Sciences.

-
- [1] T. B. Pittman, Y. H. Shih, D. V. Strekalov, and A. V. Sergienko. Phys. Rev. A **52**, R3429 (1995).
 - [2] A. F. Abouraddy, B. E. A. Saleh, Alexander V. Sergienko, and Malvin C. Teich. Phys. Rev. Lett. **87**, 123602 (2001).
 - [3] R. S. Bennink, S. J. Bentley, Robert W. Boyd. Phys. Rev. Lett. **89**, 113601 (2002).
 - [4] A. Gatti, E. Brambilla, M. Bache and L. A. Lugiato, Phys. Rev. Lett. **93**, 093602 (2004);
 - [5] M. D'Angelo and Yanhua Shih, quant-ph/0302146, <http://arxiv.org/>.
 - [6] G. Scarcelli, A. Valencia, Y. Shih, Phys. Rev. A **70**, 051802(R) (2004).
 - [7] R. S. Bennink, S. J. Bentley, Robert W. Boyd, J. C. Howell. Phys. Rev. Lett. **92**, 033601 (2004).
 - [8] A. Gatti, E. Brambilla, and L. A. Lugiato, Phys. Rev. Lett. **90**, 133603 (2002);
 - [9] A. Gatti, E. Brambilla, M. Bache and L. A. Lugiato, Phys. Rev. A **70**, 013802 (2004).
 - [10] Yangjian Cai and Shi-Yao Zhu, quant-ph/0407240, <http://arxiv.org/>.
 - [11] Yangjian Cai and Shi-Yao Zhu, Opt. Lett. **29**, 2716, (2004).
 - [12] De-Zhong Cao, Jun Xiong, and Kai-ge Wang, Phys. Rev. A **71**, 013801 (2005).
 - [13] Alejandra Valencia, Giuliano Scarcelli, Milena D'Angelo, and Yanhua Shih, Phys. Rev. Lett. **94**, 063601 (2005).
 - [14] D. Magatti, F. Ferri, A. Gatti, M. Bache, E. Brambilla and L.A. Lugiato, quant-ph/0408021, <http://arxiv.org/>.
 - [15] R. Hanbury Brown, *The intensity interferometer*, (Taylor and Francis Ltd. London 1974). See Eq. 4.26.
 - [16] Bernhard Welz, *Atomic absorption spectroscopy*, (Verlag Chemie. Weinheim. New York 1976).
 - [17] Rodney Loudon, *The quantum theory of light* (Clarendon Press, Oxford 1983).
 - [18] M. I. Kolobov, Rev. of Mod. Phys. **71**, 1539, (1999).
 - [19] R. Hanbury Brown, R. Q. Twiss. Ibid. **243**, 291, (1958).
 - [20] Jing Cheng and Shensheng Han, Phys. Rev. Lett. **92**, 093903 (2004).